Annu. Rev. Fluid Mech. 2005. 37:295–328
doi: 10.1146/annurev.fluid.37.061903.175815

THE DYNAMICAL SYSTEMS APPROACH TO LAGRANGIAN TRANSPORT IN OCEANIC FLOWS

Stephen Wiggins
School of Mathematics, University of Bristol, Bristol BS8 1TW, United Kingdom

Key Words oceanography, hyperbolic trajectory, flow barrier, invariant manifold, lobe dynamics

■ **Abstract** Chaotic advection and, more generally, ideas from dynamical systems, have been fruitfully applied to a diverse, and varied, collection of mixing and transport problems arising in engineering applications over the past 20 years. Indeed, the "dynamical systems approach" was developed, and tested, to the point where it can now be considered a standard tool for understanding mixing and transport issues in many disciplines. This success for engineering-type flows motivated an effort to apply this approach to transport and mixing problems in geophysical flows. However, there are fundamental difficulties arising in this endeavor that must be properly understood and overcome. Central to this approach is that the starting point for analysis is a velocity field (i.e., the "dynamical system"). In many engineering applications this can be obtained sufficiently accurately, either analytically or computationally, so that it describes particle trajectories for the actual flow. However, in geophysical flows (and we concentrate here almost exclusively on oceanographic flows), the wide range of dynamically significant time and length scales makes the justification of any velocity field, in the sense of reproducing particle trajectories for the actual flow, a much more difficult matter. Nevertheless, the case for this approach is compelling due to the advances in observational capabilities in oceanography (e.g., drifter deployments, remote sensing capabilities, satellite imagery, etc.), which reveal space-time structures that are highly suggestive of the structures one visualizes in the global, geometrical study of dynamical systems theory. This has been pursued in recent years through a combination of laboratory studies, kinematic models, and dynamically consistent models that have all been compared with observational data. During the course of these studies it has become apparent that a new type of dynamical system is necessary to consider in these studies (i.e., a finite time, aperiodically time-dependent velocity field defined as a data set), which requires the development of new analytical and computational tools, as well as the necessity to discard some of the standard ideas and results from dynamical systems theory. In this article we review a number of the key developments to date in this young, but rapidly developing, area at the interface between geophysical fluid dynamics and applied and computational mathematics. We also describe the wealth of new directions for research that this approach unlocks.

1. INTRODUCTION

Over the past 20 years, theory, modeling, simulation, and experiment have all confirmed that chaotic advection (Aref 1984) is a robust phenomena occurring in a wide range of flows and applications. Examples of this breadth and diversity are in the following special journal issues: Acrivos et al. (1991), Babiano et al. (1994), and Aref & El Naschie (1994). The analysis and quantification of chaotic advection fits square in the middle of the mathematical subject of dynamical systems theory, and the dynamical systems approach to transport has provided a fundamentally new framework for analyzing fluid kinematics; see Ottino (1989) for a fluid mechanical introduction and Wiggins (1992) for a mathematical introduction. To draw attention to some special circumstances arising in geophysical fluid dynamics, as well as for completeness, we give a brief description of the setting. This is covered in more detail in the references above; see also Aref (2002).

We consider the situation of a passive tracer, or particle. Active tracers, and particles with inertia, are also of great interest; however, our attention focuses on the passive case. This is the situation where the velocity of the particle is the same as the velocity of the fluid. In other words, the particle does nothing more than follow the velocity of the fluid, and it therefore instantaneously changes its velocity in response to a change in velocity of the fluid. If the velocity of the fluid is given by $\mathbf{V}_{\text{fluid}} \equiv (u(x, y, z, t), v(x, y, z, t), w(x, y, z, t))$, then the equations for the motion of the particle are given by:

$$\begin{aligned} \dot{x} &= u(x, y, z, t), \\ \dot{y} &= v(x, y, z, t), \\ \dot{z} &= w(x, y, z, t). \end{aligned} \tag{1}$$

These equations contain the answers to a number of questions that one might ask. For example, given a particle at a specific location at some initial time, where will it be at some later time? Or, given a "cloud," or "blob," or "distribution" of particles, how will it evolve throughout space over time? After obtaining the answers to these questions one may then want to know why the particle, or distribution of particles, behaved as it did during the course of their time evolution. For example, are there kinematical barriers in the flow that constrain the motion; are there regions of chaos that lead to exponential separation of particle trajectories over time. The answers to these questions can be obtained "simply" by integrating the system of ordinary differential equations given by Equation 1.

The connection to dynamical systems theory becomes even more apparent if Equation 1 is two dimensional (2D) and incompressible. In this case we have $\mathbf{V}_{\text{fluid}} \equiv (u(x, y, t), v(x, y, t)) = (\frac{\partial \psi}{\partial y}(x, y, t), -\frac{\partial \psi}{\partial x}(x, y, t))$, where $\psi(x, y, t)$ is the streamfunction. The equations for passive fluid particle motion are given by:

$$\dot{x} = \frac{\partial \psi}{\partial y}(x, y, t),$$

$$\dot{y} = -\frac{\partial \psi}{\partial x}(x, y, t), \tag{2}$$

and on first glance the dynamical systems theorist would immediately recognize these as Hamilton's equations, where the role of the Hamiltonian is played by the streamfunction. If the flow is time periodic then one would typically study Equation 2 by considering the associated 2D area preserving Poincaré map. Practically speaking, the reduction to a Poincaré map means that rather than viewing a particle trajectory as a curve in space, one views the trajectory only at discrete intervals of time (i.e., a sequence of points), where the interval of time is the period of the velocity field. The value of making this analogy with Hamiltonian dynamical systems lies in the fact that a variety of techniques in this area have immediate applications to, and implications for, transport and mixing processes in fluid mechanics (Ottino 1989, Wiggins 1992).

This has been abundantly established by Ottino and collaborators over the years (see, e.g., Horner et al. 2002, Ottino 1990, Ottino et al. 1988, 1994, Swanson & Ottino 1990). They have shown the existence of flow structures such as KAM tubes in three-dimensional (3D) flows (Kusch & Ottino 1992), Smale horseshoes (Chien et al. 1986, Khakhar et al. 1986, Leong & Ottino 1989), lobes (Horner et al. 2002), and 2D Poincaré maps of 3D flows (Fountain et al. 1998) in a variety of clever experiments. Most importantly, they showed how their existence can be used to both enhance and suppress mixing and, therefore, that they play a key role in the design and optimization of any mixing device. Today, chaotic advection and, consequently, the dynamical systems point of view of transport, is at the heart of a number of applications of immense technological importance.

However, this is a review about applying this point of view and framework for studying transport in geophysical flows (mainly oceanic flows). The success of this approach for engineering applications throughout the 1980s was a major motivating factor for moving in this direction. However, one might ask "why?" because these two fields are so vastly different. The linkage occurs through flow visualization. The geosciences have seen an explosion in data gathering technology over the past 20 years, and concurrent with that has been the development of methods for visualizing these data sets. Visualizing data obtained from current following floats and drifters and satellite and remote sensing devices show numerous localized, coherent structures ranging from major currents, like the Gulf Stream, to mesoscale phenomena, such as rings and associated vortex structures, down to a variety of submesoscale vortical features such as filaments, squirts, and mushrooms. Now a key theme of dynamical systems theory is to understand the role of localized structures in governing the motion over extended regions of space of collections of trajectories. This is certainly in the same spirit as the goals one would have for analyzing the data from a drifter release experiment. When looked at in this way one sees a remarkable synergy between the mathematical framework of dynamical systems theory and the modern experimental and observational framework of geophysical fluid dynamics, and we describe a number of examples of this below.

Once this is understood the real power of the dynamical systems approach for understanding transport issues associated with "feature- or structure-dominated" geophysical flows becomes apparent because most dynamical systems techniques do not depend on a specific analytical form of the dynamical system under consideration. Rather, they require that only certain geometrical "features or structures" be present.

Before beginning, we want to state the perspective that we take in this review. We consider oceanic flows that are 2D (usually on constant density surfaces) and mostly incompressible. At the end we mention atmospheric applications. We do not have the space to go into detail about the physics of the models that we consider. Rather, we emphasize what information, and insight, dynamical systems theory can provide about Lagrangian transport in a specific setting. An important aspect to be aware of is that during the course of much of this work the classical notion of a "dynamical system" (say, as an applied mathematician working in the subject would understand the phrase) had to undergo some significant revisions, leading to new mathematical and computational challenges that were addressed and are still a topic of much research interest.

2. EXCHANGE AND MIXING BETWEEN WESTERN BOUNDARY CURRENT AND SUB-BASIN RECIRCULATION GYRES: LABORATORY STUDIES

Western boundary currents with adjacent recirculation regions are a common feature in many parts of the world's oceans, and an understanding of the nature of the exchange of fluid between the boundary current and the recirculation region is important.

Observations from tracers, floats, and current meters, as well as geostrophic calculations, have been used to construct rough maps of the flow associated with these structures. An example of such a map [taken from Deese et al. (2002) who, in turn, derived inspiration from Johns et al. (1997)] is shown in Figure 1.

The Eulerian structure in this figure suggests that ideas from dynamical systems theory could potentially give some insight into the mechanisms governing exchange of fluid between the boundary current and the recirculation gyres, and Deese et al. (2002) studied these issues in the laboratory. They devised an experiment using a circular rotating tank with a sloping bottom and a differential lid rotation. In steady rotation the flow consists of a Sverdrup interior, a western boundary layer, and a recirculation gyre. By controlling the differential lid rotation the geometry of the recirculation gyre can be made to be either a single-recirculation gyre or a twin-recirculation gyre. A schematic of this is shown in Figure 2*a,b* for steady flow.

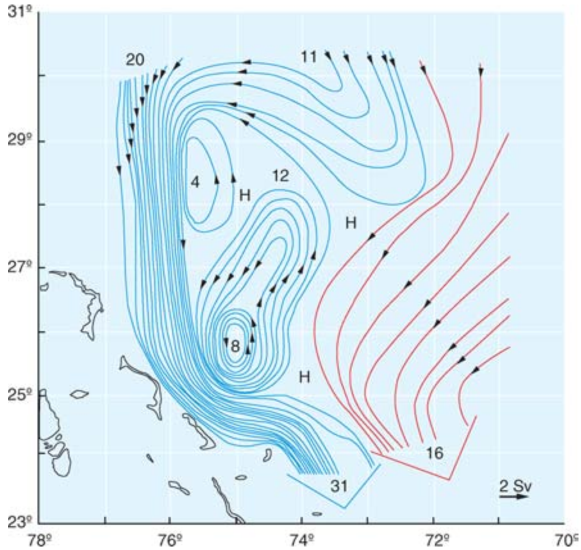

Figure 1 Figure from Deese et al. (2002) showing approximate time-averaged streamlines of the flow at about 1000-m depth associated with the North Atlantic deep western boundary current in the vicinity of Abaco Island. The contour level is 2 Sv. Deese et al. (2002) label possible locations of saddle-type (hyperbolic) stagnation points with an "H."

Time dependence of the flow can be introduced by modulating the differential rotation rate of the lid. For time-dependent flow we expect the twin-recirculation gyre to provide a novel mechanism for exchanging fluid with the western boundary current, which is schematically illustrated in Figure 2*c*.

Under weak time dependence the hyperbolic trajectory retains its saddle-point nature, in the sense of how nearby trajectories behave, but it (in general) moves in time. i.e., it is a hyperbolic or "saddle" trajectory. It also has separatrices: the stable and unstable manifolds of the hyperbolic trajectory, which also move in time. As in the steady case, the stable and unstable manifolds are material curves (so fluid trajectories cannot cross them). In the mathematician's jargon, stable (resp. unstable) manifolds are invariant. This means that the trajectory of any initial condition starting on the curve[1], must forever remain on the curve (even as the curve moves in the flow). In other words, the term invariant curve is the mathematician's manifestation of the fluid mechanician's notion of material curve. But there is a bit more to it than that. Stable (resp. unstable) manifold means that as $t \to \infty$ (resp. $t \to -\infty$) a trajectory starting on the curve not only remains on the

[1]The terminology of dynamical systems theory can often be confusing, and even misleading. For our purposes "manifold" means the same thing as "curve." The reason we retain the term "manifold" is that it is very much entrenched in the literature.

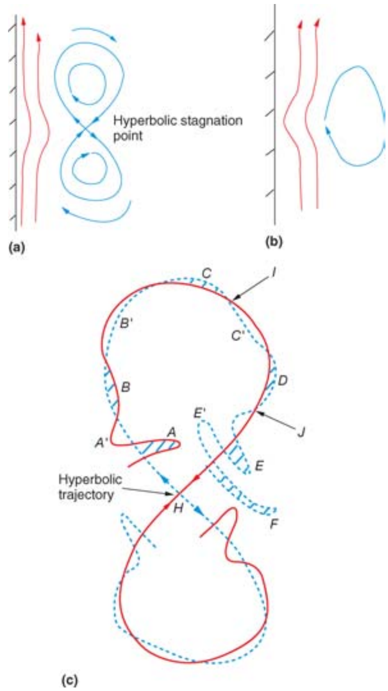

Figure 2 Figure from Deese et al. (2002) schematically illustrating the key flow structures realizable in their experiments. Panels a and b illustrate the geometry associated with a twin- and single-recirculation gyre, respectively, adjacent to a western boundary current for steady flow. Panel c illustrates the effect of unsteadiness on the twin-recirculation gyre.

curve, but actually approaches the hyperbolic trajectory in the limit $t \to \infty$ (resp., $t \to -\infty$). In this sense, the stable and unstable manifolds "spread the influence" of the hyperbolic trajectory globally throughout the flow (a discussion of this idea can be found in Beigie et al. 1994 and Malhotra & Wiggins 1998).

Contrary to steady incompressible 2D flows, if the stable and unstable manifolds of a hyperbolic trajectory in an unsteady flow intersect, they do not have to coincide. Rather, they are (typically) infinite in length and intersect at isolated points. At any fixed time these intersection points are the initial conditions of fluid particle trajectories. Because these points are in both the stable and unstable manifold of the hyperbolic trajectory the corresponding particle trajectory approaches the hyperbolic trajectory as $t \to \infty$, and as $t \to -\infty$. The segments of stable and unstable manifolds between two adjacent intersection points trap regions of fluid, called lobes. Therefore, as time evolves these lobes move toward the hyperbolic fluid particle trajectory because the intersection points of the stable unstable manifolds defining the lobe move toward the hyperbolic trajectory, dragging the segments of stable and unstable manifolds between them along in the process. As the lobes move near the hyperbolic trajectory, they feel the saddle-point influence and they are squeezed and stretched into long filaments. Spatially, the geometrical structure can appear quite complicated; however, temporally fluid particles must follow an ordered procession through this complex structure (which is inherited from the motion of the intersection points along the one-dimensional stable and unstable manifolds). This leads to the method of lobe dynamics (Malhotra & Wiggins 1998, Rom-Kedar et al. 1990, Rom-Kedar & Wiggins 1990), which we discuss in more detail below. For now, we merely describe the lobe dynamics for this problem from Deese et al. (2002).

The lobes associated with the twin-recirculation gyre are illustrated schematically in Figure 2*c*. In this figure the letters A, B, etc. denote lobes that are transported out of the northern gyre, and A′, B′, etc. denote lobes that are transported into the northern gyre. This figures illustrates the stable and unstable manifolds of the hyperbolic trajectory at a fixed time (and for a finite length of the manifolds). However, because the flow is time periodic, if one views these manifolds only at discrete intervals of time, where the time interval is the period of the flow, then for this sequence of times the manifolds are stationary. But the fluid certainly moves as time evolves. The fluid contained in a lobe at a given time must always be in a lobe at any other time. This is just another way of saying that lobes evolve into lobes. In Figure 2 lobes evolve in the following sequence as time increases: $A \to B \to C \to D \to E \to F$, which transports fluid from inside the northern gyre to outside the gyre, and $A' \to B' \to C' \to D' \to E'$, which transports fluid from outside the northern gyre to inside the northern gyre (which could then intersect lobes that would allow it to escape again).

Hyperbolic trajectories and lobes are not present in the single-recirculation gyre configuration, leading one to believe that the twin-recirculation gyre configuration is more efficient in terms of exchange with the western boundary current. This was verified by Deese et al. (2002).

Deese et al. (2002) also approximately tracked individual lobes and verified the lobe dynamics transport scenario described above. They also convincingly showed that the lobe dynamics mechanism formed the spatio-temporal template that governs transport between the western boundary layer and the recirculation gyre.

Figure 3*a* shows the result of dye injected in the western boundary current just to the west of the southern gyre. The influence of the lobe structure of the recirculation gyre is evident. Here fluid gets pulled around the outside of the recirculation gyre. Some of the fluid is in the lobes, and some follows along outside the lobes. This illustrates the fact that unstable manifolds often act as “attracting” spatial structures in a flow (Beigie et al. 1994). Figure 3*b* shows the result of dye injected just inside the edge of the southern gyre. Here fluid may be expelled from the southern gyre but only through the lobes. Parts of the exiting lobes can either circulate around the northern gyre or the lobes of the northern gyre that carry fluid into the gyre. Both behaviors occur. Finally, Figure 3*c* shows the result of dye injected well inside the southern gyre. This fluid does not escape, and this illustrates the fact that in

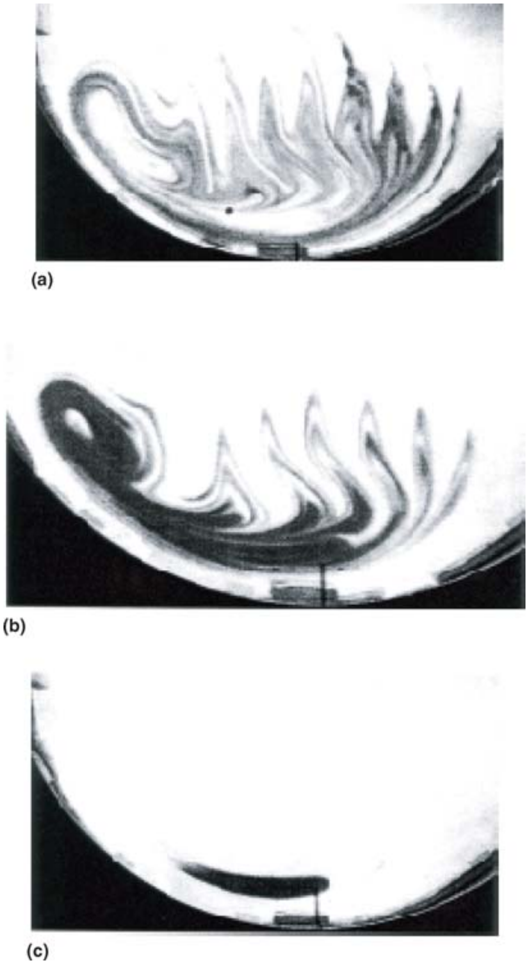

Figure 3 (*a*) The space-time evolution of dye injected very close to the western boundary of the southern gyre. (*b*) Injection just inside the edge of the southern gyre, and (*c*) corresponds to injection well inside the southern gyre. North is to the left. Figure from Deese et al. (2002).

time-periodic, or quasiperiodic, flows the interiors of gyres often contain barriers to transport that the lobes cannot penetrate.

The experimental results of Deese et al. (2002) show that ideas from dynamical systems theory play an important role in understanding the space-time structure of exchange between a western boundary current and an adjacent recirculation gyre containing a hyperbolic trajectory. It also calls into question the validity of treating the problem via the classical approach of homogeneous turbulent fluctuations superimposed on a mean flow because, even though there may be a complex stretching and folding process in the flow, transport between geometrically different flow regimes occurs at specific regions in space, and is "ordered" in time (in the sense that lobes evolve to lobes following a specific spatial order).

In another experimental/computational study related to western boundary current and adjacent gyres, Miller et al. (2002) studied transport associated with an unsteady recirculation region trapped behind a boundary. A detailed study of the influence of the stable and unstable manifolds of hyperbolic trajectories is carried out by using a numerical model to compute hyperbolic trajectories and their stable and unstable manifolds (we return to the new issues associated with these computations below). The stable and unstable manifolds allow one to rigorously define a time-dependent recirculation region, and this approach eliminates "pseudofluxes" that are created by the bulk movement of this time-dependent recirculation region past fixed boundaries. The lobes describe the "long-range transport" of fluid away from the oscillating recirculation region (Coulliette & Wiggins 2001, Malhotra & Wiggins 1998) as a spatially and temporally ordered procession of lobes around the recirculation region. A further important feature of this work is that there is another, much more well-known, transport mechanism in this problem: Ekman transport. It is natural to consider the relative importance of both mechanisms. They showed that in certain parameter regimes lobe dynamics is the dominant transport mechanism.

Many of the first applications of the dynamical systems approach to transport were concerned with kinematics. However, the study of Miller et al. (2002) is significant because it used a lobe dynamics analysis to learn something about dynamics. One particular dynamical constraint can be written as a circulation integral around the edge of the gyre. Changes in the circulation about the gyre (in Kelvin's sense) are due in part to fluxes of potential vorticity (PV) into the gyre. They show that PV is advected into or out of the gyre by lobes and they give methods to calculate this contribution explicitly.

3. TRANSPORT AND EXCHANGE PROCESSES ASSOCIATED WITH JETS

Another common structure located in various parts of the world's oceans are strong coherent currents, or jets. Examples include the Gulf Stream, Kuroshio, and the Antarctic circumpolar current. Although these jets are persistent, their spatial structure can vary a great deal over time. They can exhibit complex wave-like patterns, or meanders, or they can "fold back onto themselves" resulting in the pinching off, or shedding, of a ring-like structure. An important question is how transport near the jet is governed by these geometrical features of the jet.

3.1. Kinematic Models of Jets

In some sense Amy Bower is the mother of the dynamical systems approach to the study of transport associated with jets (Bower 1991). She developed a kinematic model of a meandering jet to explain the relationship between fluid parcel pathways and meanders of the Gulf Stream that were observed from the trajectories of 37 constant-density RAFOS floats launched in the center of the Gulf Stream near Cape Hatteras (Bower & Rossby 1989), and this model has been the inspiration for much further study. From this data, Bower & Rossby made the following observations concerning exchange of fluid between the Gulf Stream and the surrounding fluid: (*a*) fluid at the center of the Gulf Stream is most often lost from the trailing edges of meander troughs and crests, whereas entrainment occurs mainly at the leading edges of meander crests, (*b*) exchange occurs more readily in the lower main thermocline, rather than in the upper layers, and (*c*) cross-stream motions and entrainment of fluid are enhanced when the curvature of the Gulf Stream path is large.

She devised a simple kinematic model consisting of a jet of uniform width that is deformed by a sinusoidal meander propogating with a constant velocity. In a coordinate frame moving with the speed of the meander there are three qualitatively distinct types of streamline contours: (*a*) an eastward-propagating meandering jet (or "prograde" motion), (*b*) regions of recirculating fluid below and above meander crests and troughs, respectively, and (*c*) regions of westward-propagating fluid (or "retrograde" motion) above and below the jet and recirculation regions. In the classical fluid mechanics literature this is just the standard Kelvin-Stuart cat's eyes flow pattern.

Samelson (1992) reconsidered Bower's kinematic model of a meandering jet, but he made the important observation that Bower's model did not allow for exchange of fluid between the jet and its surroundings. The reason for this is that in the frame moving with the meander the flow is steady. Hence the particle trajectories are given by the contours of the streamfunction, which cannot cross. But what does this imply for Bower's work? There is an important point to understand here. Strictly speaking, her model does not allow for exchange of fluid. However, her model correctly embodied the flow structures that provide the geometrical template for exchange in a meandering jet, and reading her arguments carefully confirms this. All that was lacking was a mechanism allowing the transference of particles between these flow structures. Samelson recognized that this mechanism could be provided by inherent variability ("time dependence") in the flow. He reconsidered exchange in Bower's model, but allowed for three types of variability: (*a*) a time-periodic, spatially uniform meridional velocity superimposed on Bower's model, (*b*) a periodically time-varying meander amplitude, and (*c*) a propagating plane wave superimposed on Bower's model. Samelson considered "small-amplitude" variability so that it could be mathematically treated as a perturbation of Bower's model, and this enabled him to use a tool from dynamical systems theory, Melnikov's method (see, e.g., Wiggins 2003), to analyze the effect of small-amplitude time dependence on separatrices in time-independent systems. As described above, we typically expect the separatrices to "break apart," become infinite in length, and intersect each other in an infinite number of distinct points, giving rise to lobes and the transport mechanism of lobe dynamics. The area of a lobe is related to the amount of exchange between regions. A Melnikov function is an integral of a certain function involving pieces of the steady and unsteady velocity fields along the unbroken separatrix in the underlying steady flow. In this sense it does not require any information about particle trajectories in the unsteady flow. However, properties of the Melnikov function provide information on the intersection of the stable and unstable manifolds in the unsteady flow and the size of the lobes. Simple zeros of the Melnikov function correspond to intersection points of the manifolds, and the integral of the Melnikov function between adjacent zeros is an approximation to the area of the corresponding lobe (the error with respect to the actual area is quadratic in the size of the unsteadiness, as measured in some appropriate norm). The Melnikov function is also a function of the system parameters. Therefore one obtains a global picture in parameter space of the exchange process, as manifested through the behavior of the manifolds described above. Melnikov-type methods for aperiodic time dependence can be found in Wiggins (1988), Beigie et al. (1991), Beigie et al. (1994), and Malhotra & Wiggins (1998). Finite-time Melnikov theory is developed in Balasuriya et al. (2003).

The Bower-Samelson kinematic model of a meandering jet has inspired further analysis, e.g., Duan & Wiggins (1996), Malhotra et al. (1998), Cencini et al. (1999), and Boffetta et al. (2001), and it also provides a useful flow for benchmarking new analytical and computational methods.

3.2. Dynamically Consistent Models of Jets

The kinematic models of jets described above were criticized for not being dynamically consistent; e.g., they were not the solution of some fluid dynamical equations of motion and they did not conserve PV in the absence of dissipation. A first step in addressing these criticisms was taken by Rogerson et al. (1999), who considered transport issues associated with a meandering jet that was obtained through numerical solution of the barotropic, β-plane, PV equation, with periodic boundary conditions in the zonal and meridional directions. The flow evolves from a weakly perturbed zonal jet initial condition until it saturates to a finite-amplitude meadering state that has many of the geometrical features of the Bower-Samelson kinematic model. The meander propagates to the east at almost constant speed, and slowly decays as a result of weak dissipation. In a coordinate frame moving with the average speed of the meander one can identify the jet, recirculation regions above the troughs and below the crests of the jet, and westward-moving, or retrograde, motion, above and below these structures.

Once the dynamically consistent jet is computed over a time interval of interest, the next step is to demonstrate that it has the same mechanism for exchanging fluid as the Bower-Samleson kinematic model. However, to apply the ideas from dynamical systems theory one must surmount some mathematical obstacles. First, the velocity field obtained in this way is a finite-time data set, as opposed to a kinematic model given by an analytical formulae defined for all time. Of course, it is well established that with interpolation one can integrate particle trajectories. However, identifying hyperbolic trajectories and their stable and unstable

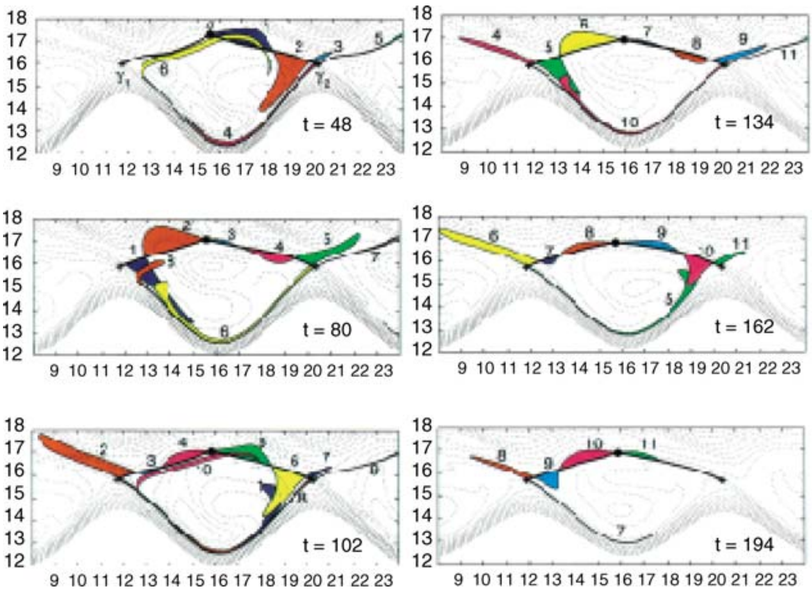

Figure 4 Figure from Rogerson et al. (1999) showing the exchange mechanism between the northern recirculation region and the northern retrograde region. The dashed contours correspond to potential vorticity.

manifolds requires new considerations, especially because traditionally, in dynamical systems theory, these are "infinite-time quantities." Suffice it to say that, for the moment, some of these difficulties have been overcome. We discuss them more fully below, but now we describe the results of Rogerson et al. (1999).

Figure 4 shows exchange between the northern recirculation region and the northern retrograde region. The points γ_1 and γ_2 denote hyperbolic trajectories at each time, and the stable manifold of γ_1 intersects the unstable manifold of γ_2 to form lobes. The boundary between the two regions is formed from a finite-length piece of the stable manifold of γ_1 and a finite piece of the unstable manifold of γ_2, and is denoted by the heavy, dark line in the figure. These evolve in time to effect exchange between these two regions in the following way: lobes 1 (purple) and 2 (red) cross the region boundary during $t \in [48, 80]$, lobes 3 (blue) and 4 (pink) cross the region boundary during $t \in [80, 102]$, and lobes 5 (green) and 6 (yellow) cross the region boundary during $t \in [102, 134]$.

The same procedure is followed to show exchange between the jet and the recirculation region, where it is found that the relevant lobes are much smaller, indicating that more exchange occurs between the northern recirculation region and the retrograde region than between the jet and the recirculation region.

Rogerson et al. (1999) also dimensionalized the quantities of fluid participating in these exchange processes in a manner appropriate for the Gulf Stream and found quantities on the order of 0.5 to 4 Sv over one meander wavelength. This is comparable to estimates of the amount of fluid transported by detaching Gulf Stream rings (a completely different transport mechanism), which is estimated at 1 to 5 Sv (where they assumed an average formation rate of 5 to 6 rings per year over distances comparable to the meander wavelength of their numerically computed jet, an average ring diameter of 130–250 Km and a thickness of 500 m).

3.3. The Relationship of "Real Drifters" to Lobe Dynamics

This work on jets described above stimulates the obvious question of how relevant geometrical structures such as hyperbolic trajectories and their stable and unstable manifolds and the associated lobes are to actual drifters in the Gulf Stream. An obvious difficulty to overcome is that all of the above studies took place in a frame moving with the (dominant) meander phase speed, and this is important because the "cat's-eye" structure would not have been apparent otherwise.

Lozier et al. (1997) used float[2] data from the 37 floats launched as part of the RAFOS Pilot Program (Bower et al. 1986) conducted between 1984 and 1985. Phase speed information during the time of the float deployment was obtained from work of Lee (1994) and Lee & Cornillon (1995), who used infrared images of the sea surface temperature from AVHRR (Advanced Very High Resolution Radiometer) to digitize the Gulf Stream path from April 1982 to December 1989. Now at any given time the Gulf Stream is characterized by a number of different meanders that move at different phase speeds and Lozier et al. (1997) developed a technique for obtaining a spatial and temporal match between a specific meander and a given float's positions (subject to a variety of criteria, which were satisfied by only 4 of the 37 floats). With this information, it is possible, for a given float, to transform to a frame moving with the appropriate meander phase velocity.

In the moving frames there was looping and oscillatory behavior, which was strongly suggestive of floats passing in and out of cat's eye–like structures. This behavior was further correlated with the stable and unstable manifolds in the numerical model of a jet described in Miller et al. (1997), after which it was concluded that crossings of critical lines (i.e., regions where the meander phase speed equals the maximum zonal velocity of the jet) are associated with lobes of fluid that move in and out if the cat's eyes. Lozier et al. (1997) also point out that the geometrical features of the lobes are reminiscent of the filaments that were observed "trailing" from Gulf Stream meander crests and troughs. It is further suggested that the thinning and stretching of lobes that results from their interaction with hyperbolic trajectories should enhance the diffusion of any properties carried by the fluid mass contained in the lobes.

The work of Lozier et al. (1997) is very significant in that it is the first study of drifters in a moving frame of reference. This was motivated by the dynamical

---

[2]"Drifter" and "float" are used synonomously.

systems approach to transport in jet models, which showed that in an appropriate moving frame there are geometrical structures that form the space-time template upon which transport occurs. It also suggests that there are situations where transport phenomena induced by the large-scale geometrical structures in the flow are not affected by small-scale turbulence.

3.4. A Barrier to Cross-Jet Transport

In our discussions of exchange for both the kinematic model and the dynamically consistent model of the meandering jet described above we have only discussed exchange between the jet and a recirculation region, or exchange between the recirculation region and a retrograde region. We have not considered exchange across the jet. There are reasons for that, which merit a separate discussion.

Strong zonal jets, in both the ocean and atmosphere, have strong barriers to transport near their centerlines. This was dramatically illustrated in a classic laboratory experiment of Sommeria et al. (1989), which was further analyzed in Behringer et al. (1991).

Samelson (personal communication, 2004) provides an intuitive description of the kinematic mechanism leading to cross-jet transport. Primary disturbances with phase speeds close to the jet speed induce persistent cross-jet flow. For the streamfunction in the moving frame, this leads to separatrices that extend across the jet, and these are a mechanism for enhanced cross-jet transport. Bower (1991) examined representative parameter values for disturbances in the upper Gulf Stream, where the jet is faster than the waves. The deeper Gulf Stream is slower, so the waves catch up; the unperturbed translating streamfunction becomes a string of cells (i.e., the cat's eyes merge) with no jet, ripe for cross-jet transport when perturbed. Strong perturbations to the jet closer to the surface can also achieve this. There is some brief discussion of this at the end of Samelson (1992). This heuristic picture for enhanced cross-jet exchange with depth was more fully developed in earlier works of Bower & Rossby (1989), Meyers (1994), and Pratt et al. (1995), and it was verified for dynamically consistent numerical models in Yuan et al. (2001, 2004).

3.4.1. POTENTIAL VORTICITY It has been noted in many examples that large gradients in PV have acted to inhibit transport. In the dynamically consistent jet models described above high PV gradients were present when the stable and unstable manifold could not intersect across the jet. In Yuan et al. (2004) it was observed that PV gradients weakend with depth, hence enabling such transport. This is consistent with the drifter observations of Bower et al. (1985) and the experimental realization of a jet in a rotating tank of Sommeria et al. (1989).

Early criticisms of chaotic advection in kinematic models focused on the fact that they did not conserve PV. There was a question of whether or not the additional constraint of PV conservation would prevent chaotic advection. Brown & Samelson (1994) examined this question in the context of 2D, vorticity-conserving, incompressible flows. They exploited techniques from integrable systems theory as well as a result of Moser on nonexistence of nonconstant analytic integrals of motion in chaotic systems to conclude that time-periodic, chaotic vorticity-conserving flows with (piecewise) analytic vorticity must have (piecewise) constant vorticity. This result is precisely stated in Brown & Samelson (1994), and it is important not to read more into it than is stated. It says nothing about 3D flows or dissipative flows. The implications for the particle trajectories of aperiodically time-dependent flow are also not entirely clear. Balasuriya (2001) builds on the approach of Brown & Samelson and studies the evolution equation for the PV gradient. For 2D PV-conserving flows he proves several results that gives constraints on flow structures. For example, he shows that the number of eddies and saddles are conserved, PV patches cannot be generated, and some types of Lagrangian and Eulerian entities are equivalent. He also considers the nonconservative case and obtains some qualitative results for the PV gradient evolution equation.

4. TRANSPORT AND EXCHANGE PROCESSES ASSOCIATED WITH A WIND-DRIVEN DOUBLE GYRE

Wind-driven gyres are a common feature in the ocean, and the subject of an extensive literature. Our purpose here is not to survey this literature, but to describe how ideas from dynamical systems theory can be used to analyze transport in these systems. The studies of exchange associated with meandering jets are relevant to this situation. An important example is the eastward-flowing Gulf Stream in the Atlantic Ocean, which can be viewed as separating a northern, counterclockwise gyre of cold fluid from a southern, clockwise, gyre of warm fluid. Exchange between these two gyres is, somehow, mediated by the jet separating them. The studies above are concerned with exchange associated with jet meanders. Building on Bower & Rossby (1989), Song et al. (1995) describe three mechanisms for transferring fluid from the jet to the surrounding fluid: ring generation, ring-jet interactions, and jet meanders.

Coulliette & Wiggins (2001) studied transport in the upper layer of a wind-driven, quasigeostrophic three-layer model in a rectangular basin geometry. Due to the latitudinal antisymmetric wind stress curl applied at the surface, the basic circulation pattern in the upper layer is a double-gyre structure separated by an eastward jet protruding into the flow from the confluence of the southward and northward western boundary currents. Driven by the strong eastward jet, the northern and southern gyres circulate counterclockwise and clockwise, respectively. Depending on the ocean-basin size and the amplitude of the wind stress curl, the ocean circulation exhibits rich time-dependent dynamics (Dijikstra & Katsman 1997). The wind stress curl, τ_0, is taken as a parameter to be varied. For a range of values the flow is temporally periodic, it undergoes a sequence of bifurcations for a narrow range of values to become (weakly) temporally chaotic, and as the wind stress curl is further increased, it becomes fully turbulent.

Coulliette & Wiggins (2001) studied the problem of intergyre transport for a range of wind stress curl values going from a temporally periodic to quasiperiodic to (weakly) chaotic flow. In all cases they found a hyperbolic trajectory on the western boundary whose unstable manifold extended into the flow (and could, in some sense, be viewed as the centerline of the jet) and a hyperbolic trajectory on the eastern boundary whose stable manifold extended into the flow. These manifolds intersected and formed lobes. Therefore, they formed a natural boundary between the southern and northern gyres, and transport between these gyres was controlled by lobe dynamics.

For the wind stress curl valued $\tau_0 = 0.165\,\mathrm{dyn/cm^2}$ a time-periodic velocity field was obtained, with a period of 151 days. Figure 5 shows the lobes created by the intersecting stable and unstable manifolds of the hyperbolic trajectories on the eastern and western boundaries, respectively, at $t = 27925$ days. In Figure 6, purple lobes are in the southern gyre along the western boundary, in the jet, and in the northern gyre. Green lobes can be seen in the northern gyre along the western boundary, just past the jet, and in the southern gyre. After one period (151 days) all

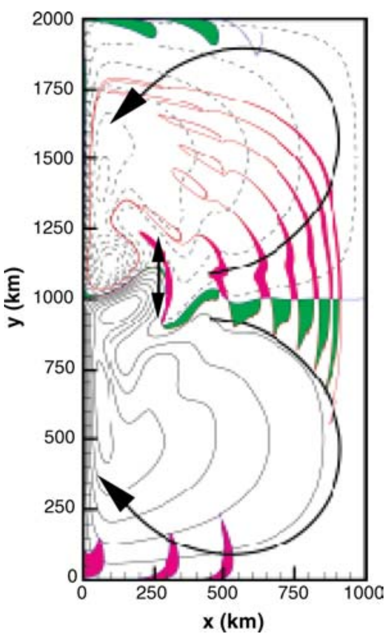

Figure 5 Lobes created by the intersection of the stable and unstable manifolds of the hyperbolic trajectories on the eastern and western boundaries, respectively, for $\tau_0 = 0.165\,\mathrm{dyn/cm^2}$ at $t = 27925$ days. To make it easier to see the lobes, they are colored with alternating green and purple. The dark arrows are laid on the figure to show the general movement of fluid in the gyres, as well as the location where fluid crosses between the gyres. Adopted from Coulliette & Wiggins (2001).

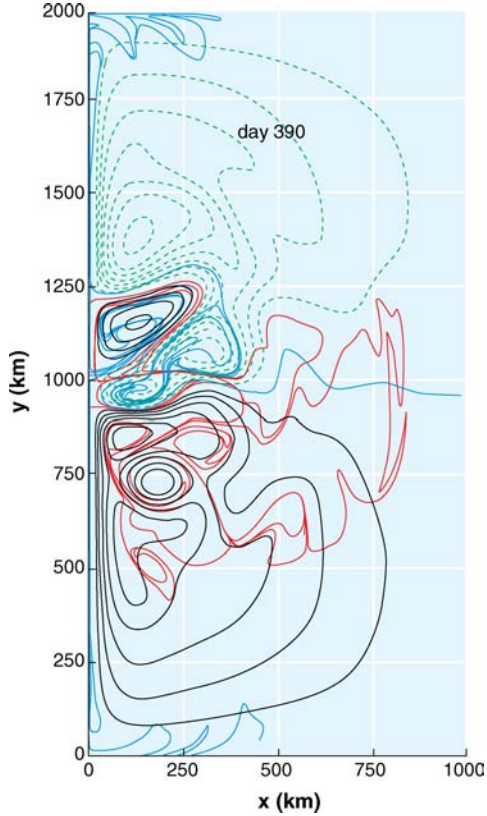

Figure 6 The unstable manifold (*red*) of the hyperbolic trajectory on the western boundary and the stable manifold (*blue*) of the hyperbolic trajectory on the eastern boundary at day 390 (after the 25,000-day spin-up from rest). The instantaneous streamlines are superimposed on the background.

of this purple fluid moves to the location of the next lobe of purple fluid immediately to the left. This conveyor belt process continues for each period. As the fluid moving from lobe to lobe (for each period) moves into the western boundary layer it is squeezed against the boundary, making it difficult to see the lobes. Lobes move up the western boundary until they are ejected into the interior of the flow by the jet. They then cross into the northern gyre, and proceed to move in a counterclockwise sense around the northern gyre. A similar conveyor belt scenario occurs for the green lobes starting in the north (remember, there are an infinite number of lobes, as the stable and unstable manifolds are infinite length, but, for obvious reasons, we can only draw a finite length, and therefore a finite number of lobes). We emphasize again that the only fluid that can cross from the southern to northern gyre (and vice versa) is through the lobes. The crossing occurs at the meander in the jet shown in the figure. All of the fluid participating in intergyre transport performs a (temporally) ordered movement in a figure-eight pattern around the southern and northern gyres, moving through the lobes. However, it can become spatially complicated by interacting with structures in the flow. In particular, the purple lobes in the northern gyre developed a ring-like structure due to the rolling up of the tips, which occurs as a result of the interaction with the eddy above the jet.

Coulliette & Wiggins also studied ring-like structures that are similar to the well-known rings often discussed in the oceanographic literature, particularly in discussions of transport processes in the vicinity of the Gulf Stream. They are similar in the sense that they are quasigeostrophic coherent Lagrangian structures, but different in that they do not have typical velocity and PV gradients associated with them. As a result, their path of travel after they are formed is simply the result of the ambient velocity field, moving slowly around the gyre, whereas rings, once they are formed, typically travel in a direction opposite to that of the ambient fluid, e.g., in the case of the Gulf Stream, they move in a direction parallel to, but opposite that of, the Gulf Stream. It is important to realize that because these rings at low τ_0 do not have associated velocity or PV gradients, they are possibly undetectable or invisible by any method other than lobe dynamics.

The next step is to extend this type of analysis to a strongly turbulent regime for the wind-driven double gyre. This only recently became possible with the development of new numerical techniques (described below). But here we show some of the hyperbolic trajectories and their stable and unstable manifolds in a turbulent regime, which indicate that the dynamical systems approach to transport can be extended to the strongly turbulent regime. Mancho et al. (2004) use the same model, but with a larger wind stress curl ($\tau_0 = 0.32\,\mathrm{dyn/cm}^2$). There are still hyperbolic trajectories on the western and eastern boundaries. In Figure 6 we show only the unstable manifold (red) of the hyperbolic trajectory on the western boundary and the stable manifold (blue) of the hyperbolic trajectory on the eastern boundary. They intersect, and are therefore the mechanism controlling intergyre transport, as described above. We still have lobes moving up and down the western boundary, into the flow along the jet, and then transferring to the opposite gyre in the process. However, one also sees a much more complex interaction of these manifolds with eddies adjacent to the jet, indicating that eddies play a role in intergyre transport.

To understand this role it is essential to compute the hyperbolic trajectories, and their stable and unstable manifolds, that are associated with the eddies because these are the structures that form the geometrical template governing the transport. In addition to the unstable manifold of the hyperbolic trajectory on the eastern boundary, and the unstable manifold of the hyperbolic trajectory on the western boundary, there are four hyperbolic trajectories in the interior with stable manifolds shown for three of them, and unstable manifolds for all four that were computed using the techniques in Mancho et al. (2004), and shown in Figure 7 on day 390 (after the 25,000-day spin-up of the flow from rest).

The stable and unstable manifolds of the hyperbolic trajectories in the interior of the flow (i.e., above and below the jet) organize the transport properties of

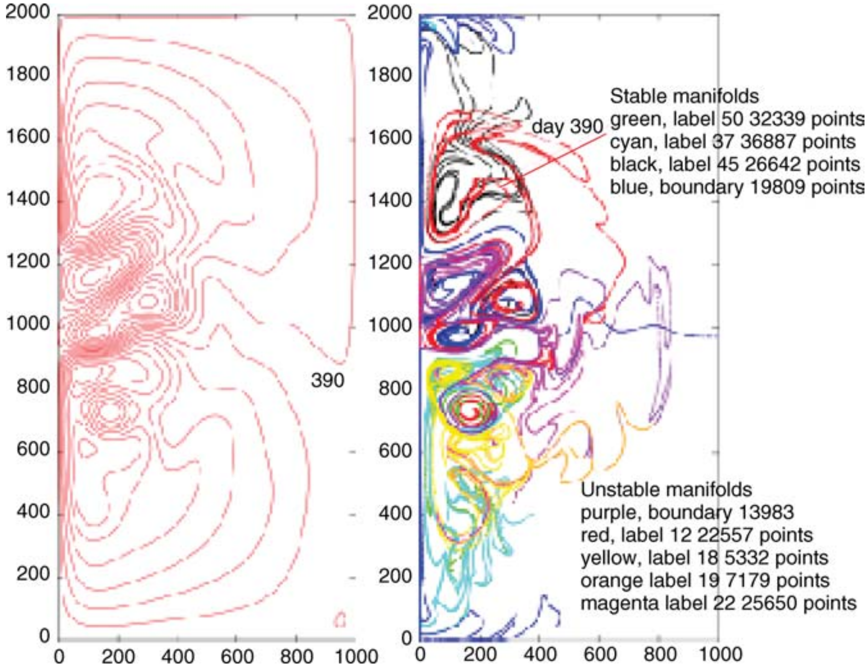

Figure 7 The left panel shows the instantaneous streamlines. The right panel shows stable and unstable manifolds for hyperbolic trajectories. The manifolds are different colors for different hyperbolic trajectories, and for whether or not they are stable or unstable manifolds. The figure also indicates the number of points that make up each manifold, and "boundary" refers to a hyperbolic trajectory on the boundary. The computation was made by Dr. A. Mancho.

eddies. Their interaction with the stable and unstable manifolds of the hyperbolic trajectories on the boundary (that are responsible for mediating intergyre transport) is complex and awaits further study. However, the hyperbolic trajectories and their invariant manifolds shown in Figure 7 indicate that turbulence modeling must go hand-in-hand with a dynamical systems–type analysis of transport. There is also a strong suggestion that this approach could also augment classical ideas of eddy-mean flow interaction.

5. MATHEMATICAL AND COMPUTATIONAL ISSUES: A NEW CONCEPT OF A "DYNAMICAL SYSTEM"

The success of the dynamical systems approach to transport and mixing in the engineering-type flows described in the introduction was accelerated by the fact that many such flows of direct importance in applications were of the type where a substantial body of mathematical and computational methods already existed.

This was due to the fact that they were either 2D and time periodic or 3D and either steady or time periodic, and either acceptable analytical formulas for the flows were available or accurate numerical techniques were available to compute the velocity fields. The Bower-Samelson model of the meandering jet falls into this situation. But once you begin to consider flows obtained by numerical solution of some dynamical equations of motion or, more generally, flows defined from data sets, fundamentally new mathematical issues arise when attempting to analyze transport in the dynamical systems framework. To begin with, this type of "dynamical system" is not a set of equations but a data set defined on a space-time grid. Second, in general we would not expect the flow to not be steady or periodic in time, i.e., it is only known for a finite-time interval and it is therefore aperiodically time-dependent (which simply means that it is not periodic). Because it is obtained as the result of a numerical computation, and therefore only available for a finite time, this poses some severe problems with applying dynamical systems–type ideas because dynamical systems theory is often described as the study of the "long time behavior" of a system. The mathematical definitions of hyperbolic trajectories, stable and unstable manifolds of hyperbolic trajectories, KAM tori, and chaos are inherently "infinite time" in nature. If we have a flow field that is only known for a finite time, and is aperiodic in time so that no inference about the behavior outside the known time interval can be made, how can we possibly proceed with a dynamical systems analysis? This is an area of continuing research, but there has been some significant progress in the area, which we describe below.

5.1. Aperiodicity in Time

Before discussing issues associated with velocity fields that are only known for a finite time it is useful to discuss some dynamical systems–type results associated with aperiodically time-dependent velocity fields that are known on an infinite-time interval. One might expect that flows that are not steady or time periodic would be very common in applications, but there has not been much work on dynamical systems analysis of transport in such flows. There are two reasons for this. One is that the emphasis of dynamical systems theory was on maps and time-periodic systems when the subject of chaotic advection began to be developed in applications. Therefore, to use the well-known theory, one had to find a system that fit the framework. This was not hard to do in many engineering applications (and still is not). The other reason is that many of the results in dynamical systems theory that are applicable to aperiodically time-dependent velocity fields were only developed in recent years and are in a rather abstract state and not so amenable to immediate usage by people not trained in the subject. Here we mention some of these results that are beginning to make their way into significant applications.

A notable exception is the notions of hyperbolic trajectories and stable and unstable manifolds of hyperbolic trajectories, which have been around for some time. We discuss these below. The notion of chaos must be given an appropriate meaning in aperiodically time-dependent systems, and this is done in Lerman &

Silnikov (1992), Meyer & Sell (1989), Scheurle (1986), Stoffer (1988a), Stoffer (1988b), and Wiggins (1999). This last reference gives the horseshoe construction for aperiodically time-dependent systems (see also Beigie et al. 1994).

5.2. Hyperbolic Trajectories

Hyperbolicity is a fundamental concept in dynamical systems theory that arises in various contexts. In continuously time-dependent systems the definition is classical and is independent of whether or not the flow is time periodic. In this review, the phrase "hyperbolic behavior" is synonomous with "saddle-point behavior." However, the dynamical systems concept of hyperbolicity is more general than this. It considers trajectories that may be either attractive or repulsive, in addition to trajectories that exhibit saddle-like behavior. It applies in three dimensions, as well as two dimensions; mathematically, it can be defined for any dimension. The fact that we are considering stability properties of a time-dependent quantity (i.e., the trajectory) means that we require more complicated mathematical tools. Some examples of why this is the case can be found in Mancho et al. (2005).

We now explain the notion of hyperbolicity for both infinite-time and finite-time velocity fields, but to be precise we need to establish some notation. Consider a velocity field:

$$\dot{\mathbf{x}} = \mathbf{v}(\mathbf{x}, t), \quad \mathbf{x} \in D, \quad t \in [t_i, t_f], \tag{3}$$

where D represents the domain of the flow and $[t_i, t_f]$ denotes the time interval on which the flow is defined. If the flow is steady or periodic in time, then it is defined for all time. If it arises from the numerical solution of some dynamical equations of motion, or it is measured experimentally, then it is only defined for a finite time (assuming it is not steady or time periodic), and it is defined on a space-time grid. Let $\bar{\mathbf{x}}(t)$ denote a general, time-evolving, trajectory of Equation 3. First, there are a few things to note that should put the situation in an appropriate context.

First, in the mathematically rigorous dynamical systems theory context, hyperbolicity properties are determined by a type of infinite-time average. This is a problem in applying the idea to Equation 3 if t_f is finite, and it is finite if the velocity field is not steady or time periodic, if it is obtained through numerical computations of some partial differential equations whose solution is the velocity field, or if it is measured experimentally. Nevertheless, we begin by giving the rigorous, infinite-time, definition of hyperbolicity because the finite-time definition follows from it naturally.

5.2.1. HYPERBOLIC TRAJECTORIES: INFINITE TIME Let $\mathbf{x} = \bar{\mathbf{x}}(t) + \boldsymbol{\xi}$, where $\boldsymbol{\xi}$ denotes the displacement from the trajectory of interest, $\bar{\mathbf{x}}(t)$. Substitute this into Equation 3, Taylor expand in $\boldsymbol{\xi}$, and retain the linear (in $\boldsymbol{\xi}$) terms:

$$\dot{\boldsymbol{\xi}} = \frac{\partial \mathbf{v}}{\partial \mathbf{x}}(\bar{\mathbf{x}}(t), t)\boldsymbol{\xi}. \tag{4}$$

This equation describes the growth of infinitesimal perturbations of the trajectory $\bar{\mathbf{x}}(t)$. It is a linear equation with time-dependent coefficients. In the general theory of (linear) ordinary differential equations such equations have two linearly independent solutions with the property that any solution is a linear combination of these two linearly independent solutions. The two linearly independent solutions make up the columns of a 2×2 matrix known as the fundamental solution matrix, denoted $\mathbf{X}(t, t_i)$, which is normalized so that $\mathbf{X}(t_i, t_i) = \mathrm{id}$, where id denotes the 2×2 identity matrix.

The Lyapunov exponents describe the "long time growth rates" of solutions of Equation 4, and the Lyapunov exponents are defined in terms of the fundamental solution matrix, as we now describe. Consider the following matrix formed from the fundamental solution matrix:

$$\mathbf{M}(t, t_i) \equiv \mathbf{X}^T(t, t_i)\mathbf{X}(t, t_i), \tag{5}$$

where the superscript "T" denotes transpose. This is a symmetric, positive definite matrix, and therefore it has two real eigenvalues. Now consider the following "infinite-time limit":

$$\mathbf{M} \equiv \lim_{(t-t_i)\to\infty} (\mathbf{X}^T(t, t_i)\mathbf{X}(t, t_i))^{\frac{1}{2(t-t_i)}}. \tag{6}$$

The Lyapunov exponents are the logarithms of the eigenvalues of $\mathbf{M}$, and they have the following interpretation. Consider an "infinitesimal" circle centered at the starting point of our trajectory, $\bar{\mathbf{x}}(t_i)$. As this circle evolves under the linearized flow about the trajectory deforms into an ellipsoid; the Lyapunov exponents are the average logarithmic expansion rates (under the flow linearized about the trajectory) of the principal axes of this ellipsoid. We say that the trajectory $\bar{\mathbf{x}}(t)$ is hyperbolic if none of its Lyapunov exponents are zero. The fundamental work on Lyapunov exponents is due to Oseledec (1968), who proves that the limit in Equation 6 exists under general conditions.

5.2.2. HYPERBOLIC TRAJECTORIES: FINITE TIME The discussion above suggests a natural generalization of the notion of Lyapunov exponents and hyperbolicity to the situation where the velocity field is defined only over a finite-time interval. We proceed exactly as in the infinite-time case. We choose a trajectory, $\bar{\mathbf{x}}(t)$, linearize about this trajectory, then solve the linearized equations for the fundamental solution matrix. With the fundamental solution matrix we form the symmetric, positive definite matrix $\mathbf{M}(t, t_i)$ as in Equation 5, and now consider the following finite-time limit:

$$\mathbf{M}(t_f, t_i) \equiv (\mathbf{X}^T(t_f, t_i)\mathbf{X}(t_f, t_i))^{\frac{1}{2(t_f-t_i)}}. \tag{7}$$

The finite-time Lyapunov exponents are the logarithms of the eigenvalues of $\mathbf{M}(t_f, t_i)$. We say that the trajectory $\bar{\mathbf{x}}(t)$ is hyperbolic on the finite-time interval $[t_i, t_f]$ if none of its finite-time Lyapunov exponents (on this time interval) are zero. In fact, if the finite-time Lyapunov exponents are given by $d_1 < 0$ and $d_2 > 0$

then it is shown in Ide et al. (2002b) that a time-dependent change of coordinates can be computed so that, in this new set of coordinates, the velocity field linearized about the hyperbolic trajectory has the form:

$$\dot{y}_1 = d_1 y_1,$$
$$\dot{y}_2 = d_2 y_2, \tag{8}$$

i.e., it is a "standard saddle," which provides even more motivation for this definition of finite-time hyperbolicity. We emphasize that this coordinate transformation, and therefore the form of Equation 8, is only valid on the finite-time interval under consideration where the finite-time Lyapunov exponents are hyperbolic, in the sense described above. It has the added advantage that the stable and unstable manifolds of Equation 8 are obvious, and these can be transformed back into the original coordinates to provide the initialization for the algorithm for computing the stable and unstable manifolds of a hyperbolic trajectory, which we describe below.

This definition of a finite-time Lyapunov exponent has been in use in the predictability community for some time (see Farrell & Ioannou 1996, Legras & Vautard 1996, Lapeyre 2002). In the ordinary differential equations community characterization of hyperbolicity is more often given in terms of exponential dichotomies (Coppel 1978, Henry 1981, or Massera & Schaffer 1966). In our context the approaches are equivalent, as shown in Ide et al. (2002b) (see also Dieci et al. 1997). Spatial distributions of finite-time Lyapunov exponents have been used to describe rapid mixing regions and barriers to transport for some years now. One of the earliest studies is that of Pierrehumbert (1991) in the context of an atmospheric transport problem. Haller (2000), Haller & Yuan (2000), and Haller (2001) developed methods for computing hyperbolic trajectories and associated material curves that are related to finite-time Lyapunov exponents and the velocity gradient tensor.

5.3. NUMERICAL COMPUTATION OF FINITE-TIME HYPERBOLIC TRAJECTORIES AND THEIR STABLE AND UNSTABLE MANIFOLDS

Various approaches have been used over the years to compute hyperbolic trajectories and their stable and unstable manifolds. There are many numerical methods that enable one to "see" saddle-point-like behavior in a flow field. The fluid particle kinematics near a saddle point is "robust" in the sense that if you initialize a blob of fluid on the saddle and let it evolve forward in time it is rapidly contracted in the stable direction and expanded in the unstable direction, and it very rapidly comes to resemble a "thickened" segment of the unstable manifold. The same procedure could be performed with time running backward to obtain an approximation of the segment of the stable manifold. Taking the intersection of these two segments at the same time gives a small region containing the hyperbolic trajectory. This rapid stretching and contraction behavior in certain regions of the flow is the foundation for a variety of numerical techniques for finding hyperbolic trajectories and their stable and unstable manifolds. However, first one must locate such hyperbolic regions.

There are several approaches for this. One is an Eulerian approach where time is frozen, and "frozen time stagnation points" or "instantaneous stagnation points" (ISPs) are examined. If the ISP is a saddle point for time frozen (fixed), then this may be a good guess for a hyperbolic region in the flow. By hyperbolic region we mean a region that contracts and stretches as it evolves in time with the flow. Deciding whether or not such a region has this property is often subjective. However, the purpose is mainly to find such a region where more refined techniques can be applied. Examples of the application of this approach can be found in Beigie et al. (1994), Malhotra & Wiggins (1998), Miller et al. (1997), Rogerson et al. (1999), Yuan et al. (2001), Yuan et al. (2004), and Poje et al. (2002).

Of course, ISPs are generally not trajectories of the velocity field, and there are situations where trying to infer actual particle trajectory information from them can lead to contradictory results (see Ide et al. 2002b for examples, as well as for a discussion of the relation between curves of ISPs and particle trajectories). However, in situations where the time variation of the velocity field is slow, then curves of ISPs may stay close to a true trajectory of the vector field. This is intuitively clear from perturbation theory and, recently, such results have been extended in Haller & Poje (1998), with an application to cross-stream mixing in a double-gyre ocean model given in Poje & Haller (1999). In the purely mathematical context related results can be found in Coppel (1978).

Ide et al. (2002b), Ju et al. (2003), and Mancho et al. (2004) introduced a method that does not require slow time variation or the location of hyperbolic regions a priori. It is based on an iteration technique in a space of curves, which, when it converges, is guaranteed to converge to a particle trajectory. Hyperbolicity is checked during each step of the convergence process. The method uses hyperbolic ISPs as an initial guess in the iterative process, but this is not equivalent to an assumption of hyperbolicity for the particle trajectories of the velocity field because ISPs are not trajectories. The curves of ISPs need not remain close to the hyperbolic trajectories that they give rise to after successful iteration.

The issue of ISPs and how they can be used to infer Lagrangian information is worthy of further investigation because they are such a prominent feature in Eulerian velocity data and are highly suggestive of Lagrangian motions. However, the relationship is extremely complex. For example, although ISPs can bifurcate, these (Eulerian) bifurcations may have no effect on (Lagrangian) hyperbolic trajectories. Examples of this can be found in Mancho et al. (2004).

Once a hyperbolic trajectory is located we want to compute its stable and unstable manifolds. In Mancho et al. (2004) the hyperbolic trajectory algorithm of Ide et al. (2002b) and Ju et al. (2003) is further developed and merged into a single, unified algorithm with the stable and unstable manifold computation algorithm described in Mancho et al. (2003). The evolution of the manifold is carried out using sophisticated numerical techniques developed by Dritschel (1989) and Dritschel & Ambaum (1997) for controlling the size of gaps between points in the manifold, interpolation, and point redistribution along the computed manifold. The numerical techniques of Dritschel and Ambaum were developed in the context of studies of the evolutions of the boundaries of vortex patches in complex fluid flows, and are ideal for the study of the evolution of stable and unstable manifolds in similar complex flows. In Figure 8 we show the unstable manifold of the hyperbolic trajectory on the western boundary computed with this algorithm. From the figure one sees that this adaptive scheme provides much more accurate manifolds and should extend the range of applications of the dynamical systems approach to more complex flows.

5.4. Mathematical Issues Associated With Dynamical Systems Defined as Finite-Time Data Sets

Computing the types of geometrical structures studied in dynamical systems theory is new and poses new challenges, especially for turbulent flows. It should also be realized that several of the fundamental concepts and results from dynamical systems theory have either no, or at best questionable, validity and usefulness when the dynamical system in question is a finite-time data set.

First, consider the notion of chaos. Although there is no universally accepted definition of the term chaos, there is general agreement about the "symptoms" that the phenomena of deterministic chaos exhibits—it occurs in a bounded region, trajectories in chaotic regions have sensitive dependence on initial conditions, and typical trajectories pass near every point in the chaotic region during the course of their evolution (see Wiggins 2003 for more precise definitions). However, most of these symptoms of chaos are infinite time in nature. Therefore, strictly speaking, chaos cannot occur in finite-time velocity fields. In numerical simulations something like chaos is observed, but there has always been a tension between numerical simulations, which are necessarily finite time, and their interpretation in the context of the infinite-time definitions and constructions of dynamical systems theory; however, this is another area where new mathematical ideas and frameworks need to be introduced. Still, one reads phrases such as "chaotic transport" defined for finite-time data sets in the developing literature of the dynamical systems approach to Lagrangian transport in geophysical flows. What is usually meant by this is the study of the transport processes using the geometrical template associated with stable and unstable manifolds of (finite-time) hyperbolic trajectories.

A new way to characterize finite-time transport in aperiodically time-dependent flows is with the idea of patchiness introduced in Mezić (1994) and Malhotra et al. (1998). The central concept is the finite-time Lagrangian velocity average, i.e., the finite-time average of the velocity field along fluid particle trajectories.

In the engineering applications mentioned in the introduction the KAM theory has played an important role because KAM tori are material surfaces in the flow that act to isolate regions and prevent them from mixing. But an important point

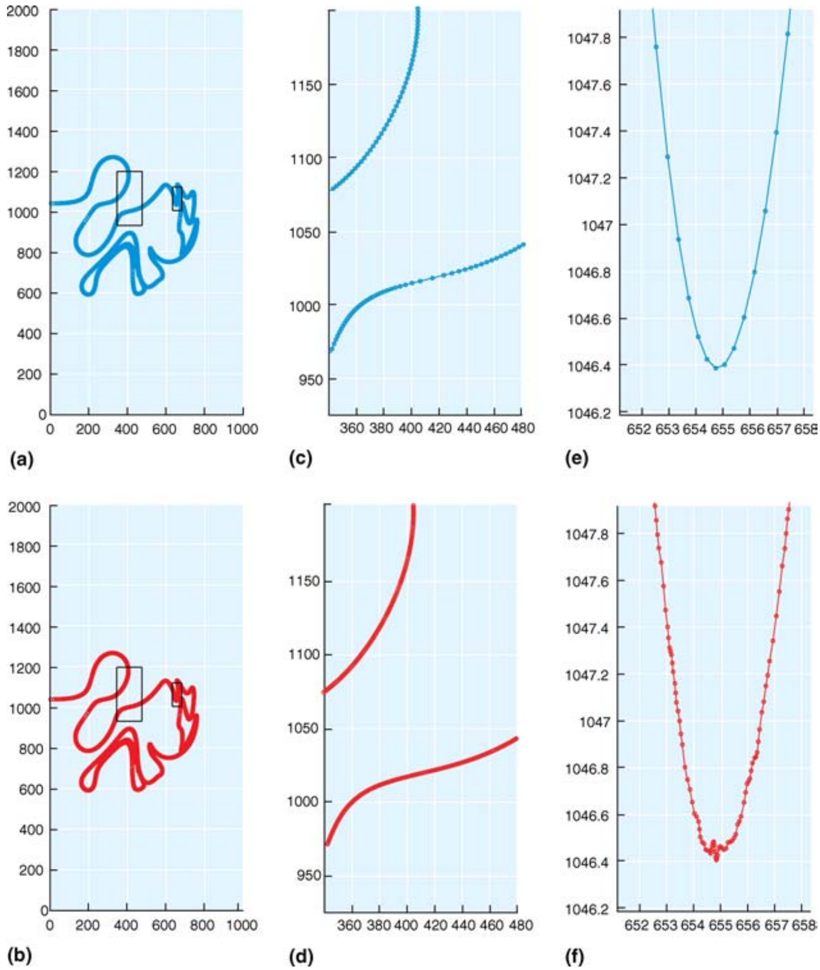

Figure 8 Figure from Mancho et al. (2004). The unstable manifold (at day 290, after the 25,000-day spin-up from rest) grown from the western boundary hyperbolic trajectory since day 50, after the 25,000-day spin-up from rest. (*a*) The global appearance of the manifold obtained with the algorithm using redistribution. The total number of points on it at this stage is 2309. (*b*) The global appearance of the manifold obtained with the algorithm without using redistribution. The total number of points on it at this stage is 7660. (*c*) A magnification of the zone marked with a big rectangle, for the manifold computed with redistribution; (*d*) the same as in (*c*) without redistribution. (*e*) A magnification of the zone marked with a small rectangle for the manifold computed with redistribution; (*f*) the same as in (*e*) without redistribution.

is that the existence of KAM tori or tubes requires either a 3D volume-preserving flow that is steady, time periodic, or time quasiperiodic, or a 2D Hamiltonian flow (i.e., given by a streamfunction) that is time periodic or time quasiperiodic. There is no KAM theorem for aperiodically time-dependent systems, or finite-time velocity fields. Therefore, the usefulness of KAM tori and tubes, indeed, their very existence, for "real ocean flows" is questionable.

Finally, we return again to the notion of hyperbolic trajectories. In the rapidly developing literature one often reads the phrases "hyperbolic trajectories disappearing after a certain time" or "bifurcation of hyperbolic trajectories." Such statements would be mysterious to a mathematician because trajectories (hyperbolic or not) cannot simply disappear, and bifurcation of trajectories only occurs when they lose hyperbolicity. Of course, the confusion lies in the term hyperbolicity, and the attempts to extend it to new settings, and retain similar terminology. In the dynamical systems literature hyperbolicity is quantified by a type of infinite-time average over the entire future of a trajectory, as we describe above. Therefore, in the classical dynamical systems sense, hyperbolicity cannot change "along a trajectory." However, the application of dynamical systems ideas to transport in geophysical flows necessitated the creation of a new concept, which is termed (for better or for worse) finite-time hyperbolicity. This is an area that is continuing to be developed.

6. OTHER WORK

It should come as no surprise that the dynamical systems approach to transport could also provide some insight into atmospheric transport problems. A recent review by Haynes (1999) discusses the role of chaotic advection in the transport of chemical species in the stratospheric polar vortex. Shepherd et al. (2000) also argue that chaotic advection is relevant to the stratosphere. Ngan & Shepherd (1997), Koh & Legras (2002), and Koh & Plumb (2000) use hyperbolic trajectories and lobe dynamics to analyze atmospheric transport problems. Winkler (2001) and Joseph & Legras (2002) provide a detailed analysis of transport in the Antarctic polar vortex from a dynamical systems point of view. They discuss the relationship between relative dispersion and invariant manifolds, as well as the implications for balloon experiments. A recently developed technique (Nakamura 1996, Winters & D'Asaro 1996) called effective diffusivity highlights some of the differences between quantifying transport in the atmosphere and the ocean. This technique can be used to quantify the effects of stirring in producing subgrid-scale property exchanges and it also can be used to locate barriers to transport. This was demonstrated in Haynes & Shuckburgh (2000a,b). Haynes & Shuckburgh (2003) studied the relationship between effective diffusivity and standard dynamical systems diagnostics and phase space structure in simple models. Deese et al. (2002) used the method to quantify transport in the laboratory model of exchange and mixing between western boundary layers and sub-basin recirculation gyres, but with much more limited success than in the atmospheric applications. The main issue is the fact that oceanographic applications require much more data coverage than is typically available—data coverage that is much more readily available to meteorologists. For example, meteorologists can measure wavenumber spectra by flying aircraft through the atmosphere. Oceanographers have to rely on satellite altimetry, which only gives the barotropic part of the circulation and is accurate only down to about 50 km or so, just when things start to get interesting (Pratt 2004, personal communication).

Lagrangian stochastic (LS) models have been used for some time to study particle trajectories in turbulent flows (see, e.g., Pope 1994, Rodean 1996). Griffa (1996) and collaborators (Buffoni et al. 1997, Dutkiewicz et al. 1993, Griffa et al. 1995, Lacorata et al. 1996) pioneered the use of LS models in oceanography. Berloff et al. (2002), Berloff & McWilliams (2002), and Berloff & McWilliams (2003) recently began a program to develop classes of LS models that can provide subgrid-scale parametrizations that will enable accurate particle tracking. A central issue here is accurate modeling of nonstationary, inhomogeneous turbulence.

Kuznetsov et al. (2002) studied transport issues associated with the loop current and the associated mesoscale rings in the Gulf of Mexico using the Colorado University Princeton Ocean Model of the Gulf of Mexico along with drifter data. They computed hyperbolic trajectories and stable and unstable manifolds and discovered detailed information about transport properties of the rings that was not available from Eulerian data. Toner et al. (2003) analyzed the transport and dispersal of plumes observed in satellite-derived ocean color images. Using dynamical systems techniques they mapped out the advective paths and determined that inter-eddy advection played a crucial role in the observed images. Notable early work on the Dutch Wadden sea was done by Ridderinkhof & Zimmerman (1992) and on the Gulf of Maine by Ridderinkhof & Loder (1994).

Poje et al. (2002) used a basin-scale, reduced-gravity model to study how drifter launch strategies affect the accuracy of Eulerian velocity fields reconstructed from the limited Lagrangian data provided by the drifters. They found that the optimal launch sites are in the regions of hyperbolic trajectories in the sense that the reconstruction error is reduced substantially compared to using randomly chosen launch sites.

7. CONCLUSIONS AND OUTLOOK

The dynamical systems approach provides a way of assessing and quantifying the effects of organized, or coherent, structures in a flow on transport. More precisely, it provides a way of giving a mathematical description to the structure, using hyperbolic trajectories, stable and unstable manifolds, lobes, etc., and a direct consequence of this description is techniques for computing flow quantities, such as fluxes. These are fundamentally new tools, as well as a new approach, for studying transport problems that are not amenable to classical approaches that draw inspiration from the turbulence theory picture of small-scale eddies giving rise to coarse-grain diffusion. Along these lines there are some possibilities that these ideas can be used to understand the dynamic linkages between localized ocean structures and large-scale ocean motions.

However, the door has really only just been opened to a wealth of problems that can now be tackled in a quantitative manner. One such area of problems arises from the important difference between geophysical fluid dynamics today, and say 20 years ago, in the shear amount of data available to researchers arising from satellite observations, high-frequency radar arrays, massive drifter deployments, and large-scale computations. Dynamical systems theory provides a unique tool for "mining" information from these large data sets. We have already seen the first (and, to date, only) example of dynamical systems theory providing new techniques for analyzing drifter data in the work of Lozier et al. (1997). There are many potential ways that the dynamical systems approach could be interfaced with satellite imagery data or other remote sensing data. The first is in the identification of critical points and geometric structures in the surface flow. Achieving this would require the development of feature models that could be "fitted" to the images and then analyzed by dynamical systems methods. This would be particularly appropriate for assessing the importance of chaotic advection. In fact, the imagery may be able to provide direct estimates of the geometric properties of lobes associated with transport. Another potential contribution of dynamical systems theory might be to quantify differences between color and thermal images.

Another important area of investigation is data assimilation using Lagrangian data. This is not such a straightforward problem because the classical data assimilation setup is inherently Eulerian. Nevertheless, some early, and very promising, work was carried out in Ide et al. (2002a), Kuznetsov et al. (2003), Ozgokmen et al. (2003), and Molcard et al. (2003). From this work one sees that the dynamical systems approach can help design data assimilation systems directly or indirectly by designing an optimal observing system (e.g., locating "good launch locations" for drifters) or by improving models for the flow fields of interest (e.g., models that include the effects of organized structures on transport).

Thinking in terms of observations and experiments, a very important area in oceanography, inverse problems, shares many themes with data assimilation that could be explored with the dynamical systems approach, for example, (*a*) estimates of oceanic fields from sparse data guided by physical laws, (*b*) estimates of meteorological forcing, (*c*) estimates of parameters in the physical laws, (*d*) design for oceanic observing systems, (*e*) resolution of mathematically ill-posed modeling problems, and (*f*) tests of scientific hypotheses.

Another theme that is emerging from the work described above is that the dynamical systems approach is providing new tools for analyzing the outputs of large-scale computations of geophysical settings. This has been one of the themes of "chaotic advection" in general. Traditionally, once the fluid mechanical equations of motion are solved you are "finished." But that is just the starting point for chaotic advection studies.

ACKNOWLEDGMENTS

I am grateful to Chris Jones, Larry Pratt, and Roger Samelson for advice and comments on early drafts of this review. It is also a pleasure to acknowledge many useful conversations with Kayo Ide, Des Small, and Ana Mancho on numerous issues related to this subject. Finally, I am very grateful to Reza Malek-Madani, Wen Masters, and Manny Fiadeiro of the Office of Naval Research not just for their financial support of this research, but also for their role in forging the links with the diverse groups in oceanography and applied mathematics that have led to the development of an essentially new approach to transport in geophysical flows. Some idea of the history behind this can be found in Jones (2000). At the beginning of this line of research the dynamical systems approach seemed far away from being able to deal with any "real problems" and the subsequent fruitful developments and collaborations are due in no small part to a number of ONR program directors taking an active role in the scientific direction of the research. This is another example of the ONR's rich legacy of visionary research support in taking the long view in supporting work whose ultimate impact and payoff can be substantial. This research was supported by ONR Grant No. N00014-01-1-0769 and the Royal Society.

The *Annual Review of Fluid Mechanics* is online at http://fluid.annualreviews.org

LITERATURE CITED

Acrivos A, Aref H, Ottino JM, eds. 1991. *Symp. Fluid Mech. Stirring Mix. Phys. Fluids A* 3(Part 2):1009–469

Aref H. 1984. Stirring by chaotic advection. *J. Fluid Mech.* 143:1–21

Aref H. 2002. The development of chaotic advection. *Phys. Fluids* 14(4):1315–25

Aref H, El Naschie MS, eds. 1994. *Chaos Applied to Fluid Mixing*. Spec. Issue *Chaos Solitons Fractals* 4:1–380

Babiano A, Provenzale A, Vulpiani A, eds. 1994. *Chaotic Advection, Tracer Dynamics, and Turbulent Dispersion. Proc. NATO Adv. Res. Workshop EGS Top. Workshop Chaotic Advection, Conf. Cent. Sereno di Gavo, Italy, 24–28 May 1993*. *Physica D* 76:1–329

Balasuriya S. 2001. Gradient evolution for potential vorticity flows. *Nonlinear Process. Geophys.* 8(4–5):253–63

Balasuriya S, Mezić I, Jones CKRT. 2003. Weak finite-time Melnikov theory and 3D viscous perturbations of Euler flows. *Physica D* 176(1–2):82–106

Behringer RP, Meyers SD, Swinney HL. 1991. Chaos and mixing in a geostrophic flow. *Phys. Fluids A* 3:1243–49

Beigie D, Leonard A, Wiggins S. 1991. Chaotic transport in the homoclinic and heteroclinic tangle regions of quasiperiodically forced two-dimensional dynamical systems. *Nonlinearity* 4:775–819

Beigie D, Leonard A, Wiggins S. 1994. Invariant manifold templates for chaotic advection. *Chaos Solitons Fractals* 4(6):749–868

Berloff PS, McWilliams JC. 2002. Material transport in oceanic gyres. Part II: Hierarchy of stochastic models. *J. Phys. Oceanogr.* 32(3):797–830

Berloff PS, McWilliams JC. 2003. Material transport in oceanic gyres. Part III: Randomized stochastic models. *J. Phys. Oceanogr.* 33(7):1416–45

Berloff PS, McWilliams JC, Bracco A. 2002.

Material transport in oceanic gyres. Part I: Phenomenology. *J. Phys. Oceanogr.* 32(3): 764-96

Boffetta G, Lacorata G, Redaelli G, Vulpiani A. 2001. Detecting barriers to transport: a review of different techniques. *Physica D* 159:58–70

Bower AS. 1991. A simple kinematic mechanism for mixing fluid parcels across a meandering jet. *J. Phys. Oceanogr.* 21:173–80

Bower AS, Rossby HT. 1989. Evidence of cross-frontal exchange processes in the Gulf stream based on isopycnal RAFOS float data. *J. Phys. Oceanogr.* 19:1177–90

Bower AS, Rossby HT, Lillibridge JL. 1985. The Gulf Stream: Barrier or blender? *J. Phys. Oceanogr.* 15:24–32

Bower AS, Rossby HT, O'Gara R. 1986. RAFOS float pilot studies in the Gulf Stream. *Univ. Rhode Island Tech. Rep.* 86-7

Brown MG, Samelson RM. 1994. Particle motion in vorticity-conserving, two-dimensional incompressible flows. *Phys. Fluids* 6(9):2875–76

Buffoni G, Falco P, Griffa A, Zambianchi E. 1997. Dispersion processes and residence times in a semi-enclosed basin with recirculating gyres: An application to the Tyrrhenian sea. *J. Geophys. Res.* 102:18699–713

Cencini M, Lacorata G, Vulpiani A, Zambianchi E. 1999. Mixing in a meandering jet: A Markovian approximation. *J. Phys. Oceanogr.* 29(10):2578–94

Chien WL, Rising H, Ottino JM. 1986. Laminar and chaotic mixing in several cavity flows. *J. Fluid. Mech.* 170:355–77

Coppel WA. 1978. *Dichotomies in Stability Theory*. *Lect. Notes Math.* Vol. 629. Berlin: Springer-Verlag

Coulliette C, Wiggins S. 2001. Intergyre transport in a wind-driven, quasigeostrophic double gyre: An application of lobe dynamics. *Nonlinear Process. Geophys.* 8:69–94

Deese HE, Pratt LJ, Helfrich KR. 2002. A laboratory model of exchange and mixing between western boundary layers and subbasin recirculation gyres. *J. Phys. Oceanogr.* 32(6):1870–89

Dieci L, Russell RD, Vleck ESV. 1997. On the computation of Lyapunov exponents for continuous dynamical systems. *SIAM J. Numer. Anal.* 34(1):402–23

Dijkstra HA, Katsman CA. 1997. Temporal variability of the wind-driven quasigeostrophic double gyre ocean circulation: basic bifurcation diagram. *Geophys. Astrophys. Fluid Dyn.* 85:195–232

Dritschel D. 1989. Contour dynamics and contour surgery: Numerical algorithms for extended, high-resolution modelling of vortex dynamics in two-dimensional, inviscid, incompressible flows. *Comp. Phys. Rep.* 10: 77–146

Dritschel DG, Ambaum MHP. 1997. A contour-advective semi-Lagrangian numerical algorithm for simulating fine-scale conservative dynamical fields. *Q. J. R. Meteorol. Soc.* 123:1097–130

Duan JQ, Wiggins S. 1996. Fluid exchange across a meandering jet with quasi-periodic time variability. *J. Phys. Oceanogr.* 26:1176–88

Dutkiewicz S, Griffa A, Olson DB. 1993. Particle diffusion in a meandering jet. *J. Geophys. Res.* 98(C9):16487–500

Farrell BF, Ioannou PJ. 1996. Generalized stability theory. part I: Autonomous operators. *J. Atmos. Sci.* 53(14):2025–40

Fountain GO, Khakhar DV, Ottino JM. 1998. Visualization of three-dimensional chaos. *Science* 281:683–86

Griffa A. 1996. Applications of stochastic particle models to oceanographic problems. In *Stochastic Modelling in Physical Oceanography*, ed. RJ Adler, P Muller, BL Rozovskii. Boston: Birkhauser

Griffa A, Owens K, Piterbarg L, Rozovskii B. 1995. Estimates of turbulence parameters from Lagrangian data using a stochastic particle model. *J. Mar. Res.* 53(3):371–401

Haller G. 2000. Finding finite-time invariant manifolds in two-dimensional velocity fields. *Chaos* 10(1):99–108

Haller G. 2001. Distinguished material surfaces and coherent structure in three-dimensional fluid flows. *Physica D* 149:248–77

Haller G, Poje A. 1998. Finite time transport in aperiodic flows. *Physica D* 119:352–80

Haller G, Yuan G. 2000. Lagrangian coherent structures and mixing in two-dimensional turbulence. *Physica D* 147:352–70

Haynes P. 1999. Transport, stirring, and mixing in the atmosphere. In *Chaos and Turbulence. Proc. NATO Adv. Study Inst. Mixing: Chaos and Turbulence, Cargese, Corse, Fr., July 7–20, 1996*, ed. H Chaté, E Villermaux, J-M Chomaz, pp. 229–72. New York: Kluwer

Haynes P, Shuckburgh E. 2000a. Effective diffusivity as a diagnostic of atmospheric transport. Part 1: Stratosphere. *J. Geophys. Res.* 105:22777–94

Haynes P, Shuckburgh E. 2000b. Effective diffusivity as a diagnostic of atmospheric transport. Part 2: Troposphere and lower stratosphere. *J. Geophys. Res.* 105:22795–810

Haynes P, Shuckburgh E. 2003. Diagnosing transport and mixing using a tracer-based coordinate system. *Phys. Fluids* 15(11):3342–57

Henry D. 1981. Geometric theory of semilinear parabolic equations. *Lect. Notes Math.* Vol. 840

Horner M, Metcalfe G, Wiggins S, Ottino JM. 2002. Transport enhancement mechanisms in open cavities. *J. Fluid. Mech.* 452:199–229

Ide K, Kuznetsov L, Jones CKRT. 2002a. Lagrangian data assimilation for point vortex systems. *J. Turbul.* 3:1–7

Ide K, Small D, Wiggins S. 2002b. Distinguished hyperbolic trajectories in time dependent fluid flows: analytical and computational approach for velocity fields defined as data sets. *Nonlinear Process. Geophys.* 9:237–63

Johns E, Fine RA, Molinari RL. 1997. Deep flow along the western boundary south of the Blake Bahama outer ridge. *J. Phys. Oceanogr.* 27:2187–208

Jones CKRT. 2000. A dynamics group looks at the ocean. *SIAM News* 33(2):1

Joseph B, Legras B. 2002. Relation between kinematic boundaries, stirring, and barriers for the Antarctic polar vortex. *J. Atmos. Sci.* 59(7):1198–212

Ju N, Small D, Wiggins S. 2003. Existence and computation of hyperbolic trajectories of aperiodically time-dependent vector fields and their approximations. *Int. J. Bifurc. Chaos* 13:1449–57

Kaper TJ, Wiggins S. 1993. An analytical study of transport in stokes flows exhibiting large scale chaos–the eccentric journal bearing. *J. Fluid Mech.* 253:211–43

Khakhar DV, Rising H, Ottino JM. 1986. An analysis of chaotic mixing in two model systems. *J. Fluid. Mech.* 172:419–51

Koh T-Y, Legras B. 2002. Hyperbolic lines and the stratospheric polar vortex. *Chaos* 12(2):382–94

Koh T-Y, Plumb RA. 2000. Lobe dynamics applied to barotropic Rossby wave breaking. *Phys. Fluids* 12(6):1518–28

Kusch HA, Ottino JM. 1992. Experiments on mixing in continuous chaotic flows. *J. Fluid. Mech.* 236:319–48

Kuznetsov L, Ide K, Jones CKRT. 2003. A method for assimilation of Lagrangian data. *Mon. Weather Rev.* 131:2247–60

Kuznetsov L, Toner M, Kirwan AD, Jones CKRT, Kantha LH, Choi J. 2002. The loop current and adjacent rings delineated by Lagrangian analysis of the near-surface flow. *J. Mar. Res.* 60(3):405–29

Lacorata G, Purini R, Vulpiani A, Zambianchi E. 1996. Dispersion of passive tracers in model flows: Effects of the parametrization of small-scale processes. *Ann. Geophys.* 14:476–84

Lapeyre G. 2002. Characterization of finite-time Lyapunov exponents and vectors in two-dimensional turbulence. *Chaos* 12(3):688–98

Lee T. 1994. *Variability of the Gulf Stream path observed from satellite infrared images*. PhD thesis. Univ. Rhode Island, Kingston, RI

Lee T, Cornillon P. 1995. Temporal variation of meandering intensity and domain-eide lateral oscillations of the Gulf Stream. *J. Geophys. Res.* 100:13603–13

Legras B, Vautard R. 1996. A guide to Liapunov vectors. In *Proc. 1995 ECMWF Sem. Predictability*, ed. T Palmer, pp. 143–56.

Leong CW, Ottino JM. 1989. Experiments on mixing due to chaotic advection in a cavity. *J. Fluid. Mech.* 209:463

Lerman L, Silnikov L. 1992. Homoclinical structures in nonautonomous systems: Nonautonomous chaos. *Chaos* 2:447–54

Lozier MS, Pratt LJ, Rogerson AM, Miller PD. 1997. Exchange geometry revealed by float trajectories in the Gulf Stream. *J. Phys. Oceanogr.* 27:2327–41

Malhotra N, Wiggins S. 1998. Geometric structures, lobe dynamics, and Lagrangian transport in flows with aperiodic time-dependence, with applications to Rossby wave flow. *J. Nonlinear Sci.* 8:401–56

Malhotra N, Mezić I, Wiggins S. 1998. Patchiness: a new diagnostic for Lagrangian trajectory analysis in time-dependent fluid flows. *Int. J. Bifurc. Chaos* 8:1053–93

Mancho A, Small D, Wiggins S. 2004. Computation of hyperbolic trajectories and their stable and unstable manifolds for oceanographic flows represented as data sets. *Nonlinear Process. Geophys.* 11(1):17–33

Mancho A, Small D, Wiggins S. 2005. A tutorial on dynamical systems concepts applied to Lagrangian transport in coastal and oceanic environments. In *Lagrangian Analysis and Prediction of Coastal and Ocean Dynamics*, ed. A Griffa, AD Kirwan, AJ Mariano, T Ozgokmen, T Rossby. New York: Academic.

Mancho A, Small D, Wiggins S, Ide K. 2003. Computation of stable and unstable manifolds of hyperbolic trajectories in two-dimensional, aperiodically time-dependent vector fields. *Physica D* 182:188–222

Massera JL, Schäffer J. 1966. *Linear Differential Equations and Function Spaces*. New York: Academic

Meyer KR, Sell GR. 1989. Melnikov transforms, bernoulli bundles, and almost periodic perturbations. *Trans. Am. Math. Soc.* 314:63–105

Meyers SD. 1994. Cross-frontal mixing in a meandering jet. *J. Phys. Oceanogr.* 24:1641–46

Mezić I. 1994. *On geometrical and statistical properties of dynamical systems: Theory and applications*. PhD. thesis. Calif. Inst. Technol., Pasadena

Miller PD, Jones CKRT, Rogerson AM, Pratt LJ. 1997. Quantifying transport in numerically generated velocity fields. *Physica D* 110:105–22

Miller PD, Pratt LJ, Helfrich KR, Jones CKRT. 2002. Chaotic transport of mass and potential vorticity for an island recirculation. *J. Phys. Oceanogr.* 32(1):80–102

Molcard A, Piterbarg LI, Griffa A, Ozgokmen TM, Mariano AJ. 2003. Assimilation of drifter observations for the reconstruction of the Eulerian circulation field. *J. Geophys. Res. Oceans* 108(C3):3056

Nakamura N. 1996. Two-dimensional mixing, edge formation, and permeability diagnosed in an area coordinate. *J. Atmos. Sci.* 53:1524–37

Ngan K, Shepherd TG. 1997. Chaotic mixing and transport in Rossby-wave critical layers. *J. Fluid Mech.* 334:315–51

Oseledec V. 1968. A multiplicative ergodic theorem: Lyapunov characteristic numbers for dynamical systems. *Trans. Moscow Math. Soc.* 19:197–231

Ottino JM. 1989. *The Kinematics of Mixing: Stretching, Chaos, and Transport*. Cambridge: Cambridge Univ. Press

Ottino JM. 1990. Mixing, chaotic advection, and turbulence. *Annu. Rev. Fluid Mech.* 22:207–53

Ottino JM, Jana SC, Chakravarthy VS. 1994. From Reynolds stretching and folding to mixing studies using horseshoe maps. *Phys. Fluids* 6(2):685–99

Ottino JM, Leong CW, Rising H, Swanson PD. 1988. Morphological structures produced by mixing in chaotic flows. *Nature* 333(6172):419–25

Ozgokmen TM, Molcard A, Chin TM, Piterbarg LI, Griffa A. 2003. Assimilation of drifter observations in primitive equation models of midlatitude ocean circulation. *J. Geophys. Res. Oceans* 108(C7):3238

Pierrehumbert RT. 1991. Large-scale horizontal mixing in planetary atmospheres. *Phys. Fluids A* 3(5):1250–60

Poje AC, Haller G. 1999. Geometry of cross-stream mixing in a double-gyre ocean model. *J. Phys. Oceanogr.* 29(8):1649–65

Poje AC, Toner M, Kirwan AD, Jones CKRT. 2002. Drifter launch strategies based on Lagrangian templates. *J. Phys. Oceanogr.* 32(6):1855–69

Pope S. 1994. Lagrangian PDF method for turbulent flows. *Annu. Rev. Fluid Mech.* 26:23–63

Pratt LJ, Lozier MS, Beliakova N. 1995. Parcel trajectories in quasigeostrophic jets: Neutral modes. *J. Phys. Oceanogr.* 25:1451–66

Ridderinkhof H, Loder JW. 1994. Lagrangian characterization of circulation over submarine banks with application to the outer Gulf of Maine. *J. Phys. Oceanogr.* 24:1184–200

Ridderinkhof H, Zimmerman JTF. 1992. Chaotic stirring in a tidal system. *Science* 258:1107–11

Rodean H. 1996. Stochastic Lagrangian models of turbulent diffusion. *Meterol. Mongr.* 26(48). Boston: Am. Meteorol. Soc.

Rogerson AM, Miller PD, Pratt LJ, Jones CKRT. 1999. Lagrangian motion and fluid exchange in a barotropic meandering jet. *J. Phys. Oceanogr.* 29:2635–55

Rom-Kedar V, Leonard A, Wiggins S. 1990. An analytical study of transport, mixing, and chaos in an unsteady vortical flow. *J. Fluid Mech.* 214:347–94

Rom-Kedar V, Wiggins S. 1990. Transport in two-dimensional maps. *Arch. Ration. Mech. Anal.* 109:239–98

Samelson RM. 1992. Fluid exchange across a meandering jet. *J. Phys. Oceanogr.* 22:431–40

Scheurle J. 1986. Chaotic solutions of systems with almost periodic forcing. *Z. Angew. Math. Phys.* 37:12–26

Shepherd TG, Koshyk JN, Ngan K. 2000. On the nature of large-scale mixing in the stratosphere and mesosphere. *J. Geophys. Res.* 105:12433–46

Sommeria J, Meyers SD, Swinney HL. 1989. Laboratory model of a planetary eastward jet. *Nature* 337:58–61

Song T, Rossby HT, Carter E. 1995. Lagrangian studies of fluid exchange between the Gulf Stream and surrounding waters. *J. Phys. Oceanogr.* 25:46–63

Stoffer D. 1988a. Transversal homoclinic points and hyperbolic sets for non-autonomous maps i. *J. Appl. Math. Phys. (ZAMP)* 39:518–49

Stoffer D. 1988b. Transversal homoclinic points and hyperbolic sets for non-autonomous maps ii. *J. Appl. Math. Phys. (ZAMP)* 39:783–812

Swanson PD, Ottino JM. 1990. A comparative computational and experimental study of chaotic mixing of viscous fluids. *J. Fluid. Mech.* 213:227–49

Toner M, Kirwan AD, Poje AC, Kantha LH, Muller-Karger FE, Jones CKRT. 2003. Chlorophyll dispersal by eddy-eddy interaction in the Gulf of Mexico. *J. Geophys. Res.* 108(C4):3105

Wiggins S. 1988. *Global Bifurcations and Chaos: Analytical Methods.* New York: Springer-Verlag

Wiggins S. 1992. *Chaotic Transport in Dynamical Systems*. New York: Springer-Verlag

Wiggins S. 1999. Chaos in the dynamics generated by sequences of maps, with applications to chaotic advection in flows with aperiodic time dependence. *Z. Angew. Math. Phys.* 50:585–616

Wiggins S. 2003. *Introduction to Applied Nonlinear Dynamical Systems and Chaos.* New York: Springer-Verlag. 2nd ed.

Winkler S. 2001. *Lagrangian dynamics in geophysical fluid flows*. PhD thesis. Brown Univ., Providence, RI

Winters K, D'Asaro E. 1996. Diascalar flux and the rate of fluid mixing. *J. Fluid Mech.* 317:179–93

Yuan G-C, Pratt LJ, Jones CKRT. 2001. Barrier destruction and Lagrangian predictabilty at depth in a meandering jet. *Dyn. Atmos. Oceans* 35:41–61

Yuan G-C, Pratt LJ, Jones CKRT. 2004. Cross-jet Lagrangian transport and mixing in a $2\frac{1}{2}$ layer model. *J. Phys. Oceanogr.* 34(9):1991–2005